Title
Structural and functional significance of water permeation through cotransporters

Journal
Proceedings of the National Academy of Sciences of the United States of America, 113(44)

ISSN
0027-8424

Authors
Zeuthen, Thomas
Gorraitz, Edurne
Her, Ka
et al.

Publication Date
2016-11-01

DOI
10.1073/pnas.1613744113

Peer reviewed

Structural and functional significance of water permeation through cotransporters

Thomas Zeuthen[a,1], Edurne Gorraitz[b], Ka Her[b], Ernest M. Wright[b,1], and Donald D. F. Loo[b,1]

[a]Department of Cellular and Molecular Medicine, The Panum Institute, University of Copenhagen, DK 2200N, Copenhagen, Denmark; and [b]Department of Physiology, David Geffen School of Medicine at University of California, Los Angeles, CA 90095-1751

Contributed by Ernest M. Wright, September 12, 2016 (sent for review August 18, 2016; reviewed by Peter Agre and Jorge Fischbarg)

Membrane transporters, in addition to their major role as specific carriers for ions and small molecules, can also behave as water channels. However, neither the location of the water pathway in the protein nor their functional importance is known. Here, we map the pathway for water and urea through the intestinal sodium/glucose cotransporter SGLT1. Molecular dynamics simulations using the atomic structure of the bacterial transporter vSGLT suggest that water permeates the same path as Na^+ and sugar. On a structural model of SGLT1, based on the homology structure of vSGLT, we identified and mutated residues lining the sugar transport pathway to cysteine. The mutants were expressed in *Xenopus* oocytes, and the unitary water and urea permeabilities were determined before and after modifying the cysteine side chain with reversible methanethiosulfonate reagents. The results demonstrate that water and urea follow the sugar transport pathway through SGLT1. The changes in permeability, increases or decreases, with side-chain modifications depend on the location of the mutation in the region of external or internal gates, or the sugar binding site. These changes in permeability are hypothesized to be due to alterations in steric hindrance to water and urea, and/or changes in protein folding caused by mismatching of side chains in the water pathway. Water permeation through SGLT1 and other transporters bears directly on the structural mechanism for the transport of polar solutes through these proteins. Finally, in vitro experiments on mouse small intestine show that SGLT1 accounts for two-thirds of the passive water flow across the gut.

water | transport | urea | SGLT1 | glucose

Water is indispensable for life as we know it, and water flow across cell membranes is central to normal physiology from single cells to complex organisms including humans. The pathways for water permeation across membranes include the lipid bilayer and water channels (aquaporins). However, it has become clear that other membrane proteins also transport water. Prominent examples are the sodium-coupled glucose and amino acid cotransporters, SGLT1 and GAT1 (1–4) and the cotransporters from the SLC12 family such as the KCC and NKCC1 (5). In this study, we focus entirely on cotransporters as water channels, i.e., the water transport induced by an osmotic gradient. Nonosmotic water transport has been reviewed (5, 6).

One feature that distinguishes cotransporters from conventional water channels, aquaporins, is that the water permeability of transporters depends on the conformational state of the protein, i.e., specific competitive inhibitors block the water pathway. For example, phlorizin blocks water permeation through SGLT1, and SKF89976A blocks water and urea permeation through the sodium-coupled GABA transporter GAT1 (3, 7). Experimental information about the water pathway through the transport proteins is not available, and the physiological significance of water permeation has not been established.

Molecular dynamic (MD) simulations using the atomic structure of the bacterial homolog vSGLT have concluded that water flows through the sugar transport pathway (8, 9), and that water permeation fluctuates because of transitions in the bulky side chains of residues forming the outer gates (10, 11). Here, we set out to challenge these conclusions by determining the importance of residues lining the sugar transport pathway in regulating water permeation. Our approach was to: (*i*) mutate selected residues lining the outer and inner gates, and the sugar binding site in human SGLT1 (hSGLT1) to cysteine (Fig. 1); and (*ii*) then measure the changes in water and urea permeability before and after chemically modifying the charge and bulk of the side chains with methanethiosulfonate (MTS) reagents. Urea transport by hSGLT1 was used to study the specificity of the water channel and, in some cases, as a surrogate tracer for water permeation.

The physiological importance of osmotic water flow through SGLT1 was determined by measuring the contribution of SGLT1 to passive water flow across the intestine, a tissue without significant expression of aquaporins.

The data support the MD conclusions that water permeation through SGLTs occurs through the sugar transport pathway, and that water:sugar:Na^+:protein interactions are at the core of the mechanism of sodium/glucose cotransport. In addition, the data underscore that SGLT1 provides a major pathway for passive water flow across the intestine.

Results

Water and Urea Permeability of Mutants in the Sugar Pathway. The water permeability of oocytes expressing hSGLT1 was measured by optically recording the changes in cell volume in response to an osmotic challenge (Fig. 2*A*). Fig. 2*B* shows a representative experiment on an oocyte expressing the hSGLT1 mutant F453C. The oocyte (volume ~1 μL) is initially bathed in an isotonic NaCl buffer. When the bathing solution was made hypertonic with the addition of 20 mM mannitol, the oocyte volume decreased, at

Significance

Transport of water and polar solutes across membranes play an important physiological role, and it is widely appreciated that many membrane transport proteins are permeable to water. Molecular dynamics studies of sodium-coupled glucose cotransporters (SGLTs) indicate that water flows through the sugar transport pathway. We test this hypothesis by mutating residues lining the sugar transport pathway through SGLT1, and measuring the changes in the permeability of water and urea before and after their chemical modification. Mutation of outer and inner gate residues and residues involved in sugar binding confirms that water and urea permeate the glucose transport pathway, suggesting that water is involved in sugar transport. SGLT1 is physiologically important in determining osmotic flow across the small intestine.

Author contributions: T.Z., E.M.W., and D.D.F.L. designed research; T.Z., E.G., K.H., and D.D.F.L. performed research; T.Z., E.G., K.H., E.M.W., and D.D.F.L. analyzed data; and T.Z., E.M.W., and D.D.F.L. wrote the paper.

Reviewers: P.A., Johns Hopkins Bloomberg School of Public Health; and J.F., Columbia University, CONICET.

The authors declare no conflict of interest.

[1]To whom correspondence may be addressed. Email: ewright@mednet.ucla.edu, tzeuthen@sund.ku.dk, or dloo@mednet.ucla.edu.

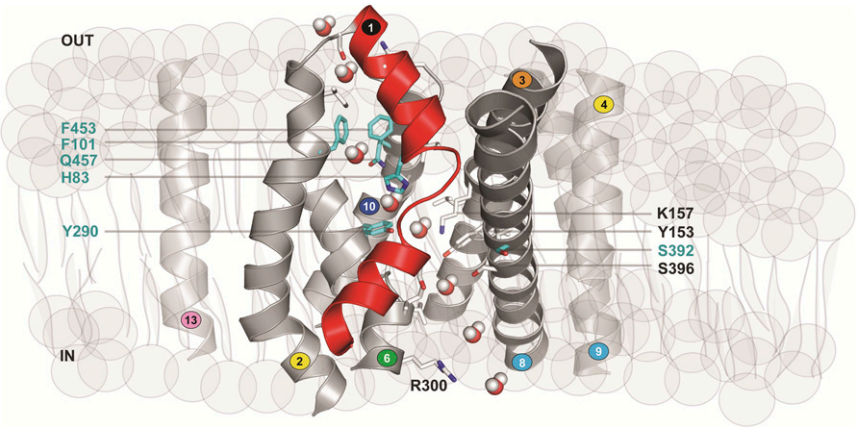

Fig. 1. Homology model of hSGLT1. The model is based on the vSGLT structure (ref. 24; Protein Data Bank ID code 3DH4) and shows the postulated water pathway through the protein. TM5, TM7, TM11, and TM12 are removed for clarity. The location of the residues mutated, H83, F101, Y153, K157, Y290, F453, Q457, S392, and S396, are indicated. Residue G507, situated on the external membrane surface of TM11, is used as a control. Circled numbers refer to the transmembrane helixes.

the rate of 40 pL·s^{-1}. Addition of phlorizin to the bathing solution reduced the volume flow to 20 pL·s^{-1}. Because phlorizin reduced the osmotic water permeability (P_f) to that of the native oocyte (3), the phlorizin-inhibited rate of volume decrease, 20 pL·s^{-1}, is the volume flow mediated by mutant F453C.

The water permeability per SGLT1 molecule was obtained by dividing the phlorizin-sensitive P_f by the density of transporters in the oocyte membrane. The results for wild-type (WT) hSGLT1 and mutants H83C, Q457C, F453C, Y290C, and G507C are shown in Fig. 3*A*. For mutants F453C and Q457C, located near the external surface of transmembrane helix 10 (TM10; Fig. 1), the unitary P_f values were significantly (~twofold) higher than for WT. For mutants H83C and Y290C, which are deeper into the sugar binding pocket (Fig. 1), the unitary P_f values were similar to WT. In the case of G507C, located on the external surface of TM11 and not in the sugar pathway, the unitary P_f was the same as WT.

The urea permeability per SGLT1 molecule (P_{urea}) of the mutants mirrors the water permeability and is shown in Fig. 3*B*. For WT and mutant Q457C, P_{urea} was 1.3 ± 0.3 and 8 ± 1.4 × 10^{-18} cm^3·s^{-1} respectively, compared with P_f values of 260 ± 40 and 420 ± 50 × 10^{-18} cm^3·s^{-1}. F453C and Q457C showed a significant increase (~twofold) in unitary urea permeability compared with WT, whereas P_{urea} was similar to WT for Y290C and H83C. The increases in P_f and P_{urea} by mutants F453C and Q457C indicate the F and Q side chains are in both the water and the urea pathways.

Effect of MTS Reagents. The effect of 2-aminoethyl methanethiosulfonate hydrobromide (MTSEA) on water transport is illustrated in Fig. 2*C* for an oocyte expressing the mutant Y290C.

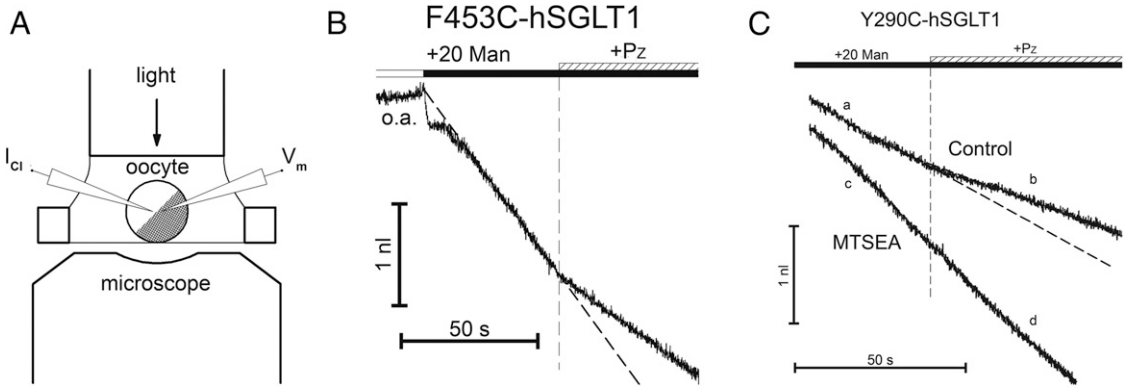

Fig. 2. Measurement of oocyte osmotic water permeability. (*A*) Changes in oocyte volume were monitored by using an inverted microscope with light supplied from a Perspex rod on top of the oocyte. The rod also served as the upper limitation of the chamber. The cross-section area of the oocyte was sampled at 25 Hz, and the calculated volume was monitored continuously. The oocyte membrane potential (V_m) was held at −50 mV by using the two-electrode voltage clamp, and the holding current (I_{hold}) was recorded (data not shown). The volume of the experimental chamber was 30 μL, and continuous perfusion was such that the bathing solution was completely replaced every 5 s. The noise level of the volume recordings was 20 pl, i.e., 0.002% of the oocyte volume of 1 μL (19). (*B*) Representative experiment on an oocyte expressing the mutant F453C. Upon addition of mannitol (20 mM) to the external solution (150 mM NaCl buffer), the oocyte began to shrink. Initially, there was a transient optical artifact (o.a.) induced by the change in optical index of the bathing solution caused by the mannitol (33). This transient was followed by a linear volume loss equivalent to 40 pL·s^{-1}. Addition of phlorizin (+Pz, 150 μM) to the external solution reduced the rate of shrinkage to that of the native noninjected oocytes (20 pL·s^{-1}). The difference in volume flow in the presence and absence of phlorizin is defined as the water flow through SGLT1. (*C*) Osmotic water flows for an oocyte expressing Y290C were determined as in *A*. The upper trace shows the volume of an oocyte expressing mutant Y290C exposed to an extracellular hyperosmolarity of 20 mOsm (black bar). The oocyte volume decreased at a rate of approximately 20 pL·s^{-1} (a). Phlorizin reduced the shrinkage rate to 10 pL·s^{-1} (b). The lines were obtained by linear regression. Subsequently, the same oocyte was washed in Pz-free NaCl buffer and incubated for 2 min in 100 μM MTSEA in NaCl buffer and the experiment was repeated. The lower trace shows that after MTSEA treatment, the oocyte volume decreased twice as fast, 40 pL·s^{-1} (c). Phlorizin had no effect on the P_f of the MTSEA-treated oocyte (d). We note that MTSEA had no effect on resting oocyte volume, as both traces originate from the same starting volume (~1 μL); in the figure, the traces have been shifted for clarity.

Before treatment by MTSEA, the volume of the oocyte decreased when mannitol (20 mM) was added to the external NaCl buffer, and phlorizin reduced the rate of cell shrinkage by 30%. After MTSEA treatment, the rate of oocyte volume shrinkage increased 100%, due to an increase in the osmotic water permeability of the MTSEA-treated Y290C, and phlorizin did not block the water permeability. MTS reagents did not affect the water permeability of native oocytes (Table 1).

Fig. 4*A* shows a graphical summary of the effects of MTSEA and 2-((5(6)-tetramethyl-rhodamine) carboxylamino) ethyl methanethiosulfonate (MTS-TAMRA) on the water permeability of Y290C oocytes. Phlorizin blocked the P_f of the Y290C-expressing oocytes to the level of the noninjected oocytes (dashed line). After MTSEA or MTS-TAMRA treatment, the P_f of the oocytes (due to SGLT1) increased 100%. Phlorizin was unable to block the water permeability of the oocytes after treatment by the MTS reagents because it is unable to interact with the protein when the sugar binding vestibule is occupied by the MTS reagent. The effect of MTSEA was largely reversed by 10 mM DTT because the P_f of the oocyte was not significantly different from that before MTSEA treatment. Similar effects of the MTSEA reagents were observed on the water permeability of mutant H83C (Table 1).

Fig. 4*B* shows the effects of MTS reagents on P_{urea} in Y290C-expressing oocytes. MTSEA significantly increased P_{urea} versus the nontreated oocytes, but MTS-TAMRA reduced P_{urea}. Thus, for mutant Y290C, MTSEA increased both water and urea permeability. After treatment with the MTS reagents, there was no significant effect of phlorizin on P_{urea}, as observed for P_f. For mutant H83C, there was no significant effect of the MTS reagents on the urea permeability (Table 2) in contrast to the effects on the water permeability (Table 1).

The effect of MTS reagents on P_f of the outer gate mutant F453C is shown in Fig. 5*A*. MTSEA did not alter P_f, and after treatment by MTSEA, phlorizin blocked the P_f. Treatment by the bulkier MTS-TAMRA resulted in a significant reduction in the P_f, and phlorizin was unable to block the remaining water permeability. Fig. 5*B* shows the effect of MTS reagents on P_{urea}. After MTSEA, there was a small but significant decrease, whereas after MTS-TAMRA, there was a larger decrease (similar to that recorded for P_f; Fig. 5*A*). Similar results were observed for the effect of MTS-TAMRA on the water and urea permeability of mutant Q457C (Tables 1 and 2). MTS reagents also decreased P_{urea} for T287C and F101C, but the effects on F101C were not significant (Table 2).

In control experiments on both native (noncRNA injected) and G507C-expressing oocytes (residue 507 is not in the sugar pathway), neither MTSEA nor MTS-TAMRA had any measureable effect on water permeability (Table 1) or urea permeability (data not shown).

Selectivity of Water Permeation. We examined the selectivity of the hSGLT1 water pathway by comparing the permeability of water, urea, and mannitol. For WT and mutant Q457C, the unitary P_{urea} values (per SGLT1 molecule) were $1.3 \pm 0.3 \times 10^{-18}$ $cm^3 \cdot s^{-1}$ and $8 \pm 1.5 \times 10^{-18}$ $cm^3 \cdot s^{-1}$. The corresponding unitary P_f values were 260 ± 40 and $420 \pm 50 \times 10^{-18}$ $cm^3 \cdot s^{-1}$ (Fig. 3). Thus, the ratio (P_f/P_{urea}) of the unitary water and urea permeability was between 50 and 200. The permeability of mannitol was insignificant for WT and mutant Y290C, and was insensitive to phlorizin (data not shown and ref. 7). These results show that the selectivity of the hSGLT1 water channel is as follows: water >> urea >> mannitol.

Water Transport Across the Intestine. To determine the contribution of SGLT1 to osmotic water flow across the intestine, we measured passive water transport across sacs of the everted mouse small intestine at 22 °C (Fig. 6*A*). The top trace of Fig. 6*B* shows that with 150 mM NaCl buffers on the internal (serosal) and external (mucosal) compartments (●), there was no significant net water flow across the intestine ($0.16 \pm 0.27 \times 10^{-3}$ $\mu L \cdot min^{-1}$). On the addition of 100 mM mannitol to the external solution (o), water flowed out of the sac into the external solution at a rate of $1.76 \pm 0.15 \times 10^{-3}$ $\mu L \cdot min^{-1}$. In another experiment shown below (▼), the same osmotic gradient (100 mOsM) produced a flow of $1.2 \pm 0.2 \times 10^{-3}$ $\mu L \cdot min^{-1}$, and after the addition of phlorizin (200 μM) to the external solution (Δ) the flow decreased to $0.1 \pm 0.2 \times 10^{-3}$ $\mu L \cdot min^{-1}$. In six experiments, phlorizin significantly reduced the osmotic water flow 65% from -19.5 ± 2 to $-6.5 \pm 2 \times 10^{-3}$ $\mu L \cdot min^{-1}$ ($P < 0.001$).

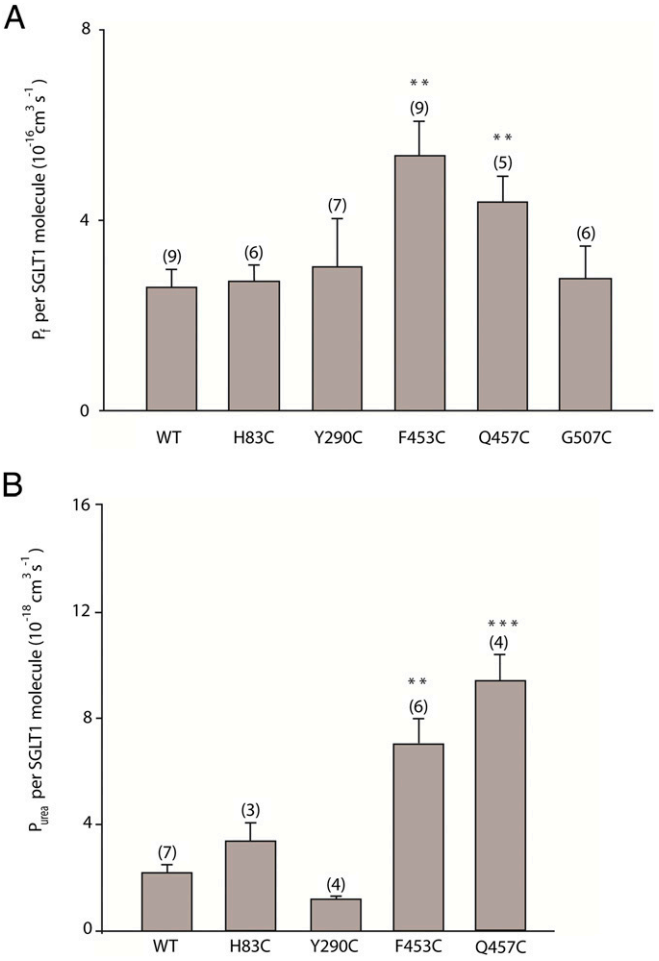

Fig. 3. P_f and P_{urea} of WT hSGLT1 and mutants. (*A*) P_f per SGLT1 molecule for WT, and mutants H83C, Y290C, F453C, Q457C, and G507C. The errors represent the SEM. The number (*n*) of experiments is indicated by the numbers above the vertical bar. ** denote statistically significance ($P < 0.01$) compared with WT measured on the same batch of oocytes. (*B*) P_{urea} per SGLT1 molecule for WT and mutants H83C, Y290C, F453C, and Q457C. SGLT1-specific P_{urea} was obtained from phlorizin-sensitive urea uptakes, $J = P_{urea} S/n \times [urea]$. [urea] is the urea concentration, *n* is the number of SGLT1 transporters in the oocyte plasma membrane determined from Q_{max} measurements, and *S* is the oocyte surface area (24). In urea experiments performed on WT and Q457C oocytes, the number of transporters expressed in the membrane was first determined in 18 oocytes by using presteady-state currents and then the urea uptakes (pmoles per oocyte/h) were measured in nine oocytes in the absence and nine oocytes in the presence of phlorizin. The number of experiments is indicated above the vertical bar. For each experimental condition, nine oocytes were used. $^{**}P < 0.01$; $^{***}P < 0.001$.

Table 1. Effects of MTS regents on P_f of oocytes expressing hSGLT1 proteins P_f (10^{-4} cm·s^{-1})

Expt	Na^+	Pz	MTSEA	MTSEA+Pz	MTS-TAMRA	MTS-TAMRA+Pz
Native	0.9 ± 0.1	0.9 ± 0.1	0.9 ± 0.1	0.9 ± 0.1	0.9 ± 0.1	—
F453C	1.2 ± 0.1	0.6 ± 0.1**	1.2 ± 0.1	0.7 ± 0.2**	1.0 ± 0.2**	1.0 ± 0.2**
Q457C	1.5 ± 0.1	0.9 ± 0.1**	1.3 ± 0.1*	1.0 ± 0.1**	1.0 ± 0.1**	1.0 ± 0.1**
H83C	1.5 ± 0.1	1.2 ± 0.1**	2.0 ± 0.2**	1.8 ± 0.2**	1.7 ± 0.1**	1.9 ± 0.2**
Y290C	1.4 ± 0.1	1.1 ± 0.1**	2.0 ± 0.2**	2.0 ± 0.1**	2.0 ± 0.1**	1.8 ± 0.1**
G507C	1.2 ± 0.1	1.0 ± 0.1**	1.2 ± 0.1	1.0 ± 0.1**	1.2 ± 0.1	1.0 ± 0.1**

Effects of MTS reagents on water permeability per oocyte (P_f). The experiments are as described in Figs. 2, 4*A*, and 5*A*. In each experiment, the contribution of SGLT1 to the total oocyte water permeability was obtained from the phlorizin-sensitive component. Each estimate is the mean ± SEM of experiments on 3–18 oocytes per clone, see Fig. 4*A* for Y290C and Fig. 5*A* for F453C. Native data were from noninjected oocytes. ** statistically highly significant from control conditions (Na^+) with $P < 0.01$; * statistically significant $P < 0.05$.

Discussion

SGLT1 has been shown to behave as a water and urea channel (1–3, 7, 12, 13). The osmotic water permeability (P_f), 2.6×10^{-16} cm^3·s^{-1} per SGLT1 protein, is approximately 1% of that for a single aquaporin (AQP1) (5.6×10^{-14} cm^3·s^{-1}). The water permeability, independent of the size and direction of the osmotic gradient, is inhibited by phlorizin with a K_i similar to that for inhibition of Na^+/glucose cotransport. The P_f is the same in the presence and absence of glucose, indicating that the water channel is preserved under sugar transporting conditions. The activation energy (E_a) for passive water and urea flow, ~5 kcal·mol^{-1}, is close to that for water permeation through aquaporins (14).

Passive water transport is a property of several types of animal and plant transporter proteins (3, 15–20) and MD simulations also suggest that water permeation is a common feature of membrane proteins (10). Likewise, a number of cotransporters have been shown to be passive urea transporters, suggesting that urea and water channels are a constitutive property of this class of membrane proteins (7, 20). However, there are exceptions in that ion transporters in the SCL12 family (KKC, NKCC1, and NKCC2) have no apparent passive water permeability (5, 21).

The unitary water permeability P_f of the hSGLT1, 2.6×10^{-16} cm^3·s^{-1} (Fig. 3*A*), is in good agreement with a previous estimate of 4.5×10^{-16} cm^3·s^{-1} for rabbit SGLT1 (12). A recent paper reports a value of 7×10^{-13} cm^3·s^{-1}, three orders of magnitude larger (22). However, it is difficult to interpret the relevance of these data, partly because the data were obtained at 5 °C and the high water permeability was insensitive to phlorizin. We also note that our estimate of the unitary P_f of AQP1 in oocytes is close to that reported for AQP1 reconstituted in liposomes (12).

MD simulations of the vSGLT crystal structure (PDB ID code 3DH4; ref. 23) indicated water flows through the sugar pathway (8–11). In the crystal structure, the sugar transport pathway is occluded from the external membrane surface by hydrophobic outer gates (M73, Y87, and F424 in the vSGLT structure; the corresponding residues in hSGLT1 are L87, F101, and F453, respectively; ref. 24). According to MD simulations, the water-conducting states of vSGLT are gated by transient spontaneous local conformational changes of the side chains of the gating residues, M73, Y87, and F424 (10, 11). Our results (Tables 1 and 2 and Fig. 5) indicate that in hSGLT1, the outer gate residue F101C has no remarkable effect on urea permeability, whereas replacing the side chain of the outer gate residue F453 with cysteine significantly increases P_f and P_{urea}, and this increase is reduced after labeling with MTS-TAMRA (Fig. 3 and Tables 1 and 2). The urea permeability of the third gate residue L87C was not measurable because of the low expression of the protein in the oocyte membrane (24). It should be noted that our assays were made on the outward-facing Na^+-bound conformation, and with a time resolution less than nine orders of magnitude lower than the MD simulations.

To map the water pathway through hSGLT1, we have examined water and/or urea transport by the cysteine mutants of residues in the sugar binding site (H83C, T287C, and Q457C), the inner gate (Y290C), and outer gates (F101C and F453C). We have furthermore chemically modified these cysteine side chains with reversible alkylating reagents. Previous studies documented the importance of these side chains in Na^+ and sugar binding and transport (24–26).

In general, our findings are consistent with the hypothesis that water, and urea, permeate through the sugar pathway. The urea uptake experiments thus provide a parallel and independent measurement of permeation through the water pathway. Water and urea permeability is either increased by the cysteine mutations (F453C and Q457C) and/or changed by alkylation of the cysteines with MTS reagents (MTSEA and MTS-TAMRA; Tables 1 and 2). The increase in water/urea permeability for F453C and Q457C may be due to the cysteine side chain offering less steric hindrance to water and urea movement than phenylalanine (F at residue 453) and glutamine (Q at residue 457). This finding agrees with the reduction in water/urea permeability when the cysteines are modified by the bulky MTS-TAMRA (Fig. 5 and Tables 1 and 2). With MTS-TAMRA attached to residues F453C and Q457C, phlorizin is unable to bind to the transporter (Fig. 5). For outer gate mutant F101C, we only have data for urea. Here, there was no increase in permeability above wild type, and only partial inhibition by MTS-TAMRA. This finding suggests that the side chain of residue F101 does not play a major role in urea permeation, but suggests that the water pathway in the outward-facing Na^+-bound conformation is lined by the side chains of F453 and Q457 on TM10.

For the three mutants deeper in the sugar binding pocket, H83C, T287C, and Y290C, there was no increase in water and urea permeability. The MTS reagents actually increased the water permeation through H83C and Y290C (Fig. 4 and Tables 1 and 2). MTSEA also increased urea permeation (not significant for H83C), and MTS-TAMRA largely blocked P_{urea}. Because the sugar pathway is obstructed by the MTS reagents, the increases in water and urea permeation (for mutants H83C and Y290C) do not appear simply due to alterations in the size of the side chains, but instead are the result of an increase in conformational flexibility. Although T287C is not involved in sugar binding, alkylation reduces urea permeation and blocks sugar transport.

Finally, in control experiments on residues not in the sugar pathway, such as G507, located in the external surface of TM11, we found that MTS reagents produced no changes in water/urea permeation (Tables 1 and 2) or sugar transport (27).

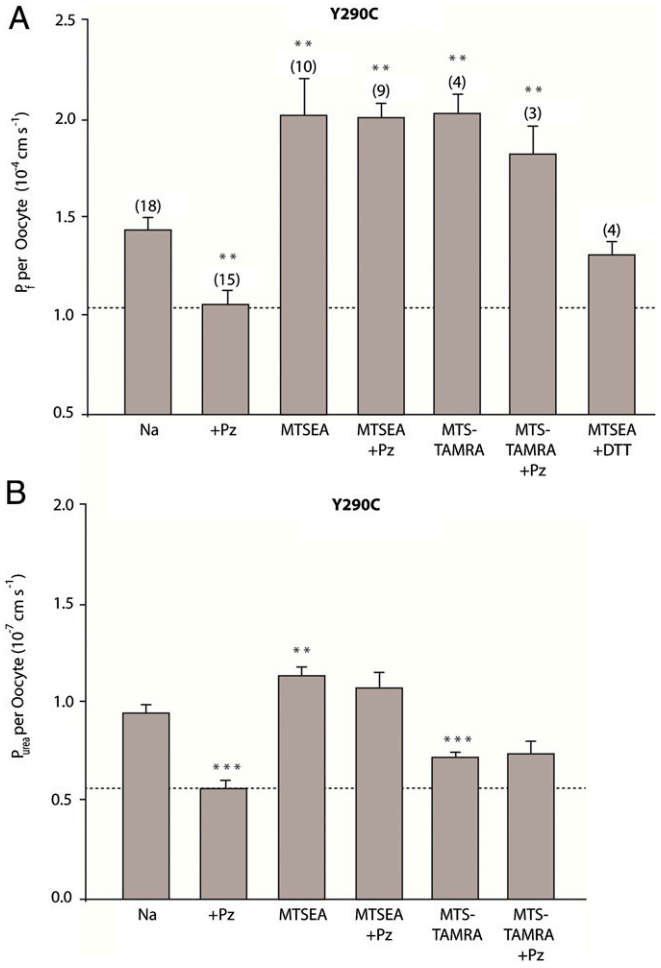

Fig. 4. Effect of MTS reagents on P_f and P_{urea} of oocytes expressing Y290C. (*A*) Effect of MTS reagents on the P_f of Y290C-expressing oocytes. Phlorizin significantly reduced the P_f to those of native oocytes (dashed horizontal line). MTSEA and MTS-TAMRA significantly increased the P_f above that of control oocytes. As tested in paired experiments, phlorizin had no significant effects on the MTSEA- or MTS-TAMRA–treated oocytes. Incubation in DTT (10 mM for 10 min) reversed the effect of MTSEA. Note that the abscissa is truncated at 0.5. ** denotes $P < 0.01$ between the experimental condition and the oocyte before MTS treatment. (*B*) Effect of MTS reagents on P_{urea} of oocytes expressing mutant Y290C. The data were obtained from a representative single experiment with nine oocytes used for each condition. The oocytes were incubated for 2-min in 100 μM MTSEA, or 1 h in 100 μM MTS-TAMRA in the presence (+) and absence of 250 μM phlorizin. *t* test shows a significant ($P \leq 0.05$) increase in P_{urea} MTSEA-treated versus nontreated oocytes, and a significant ($P \leq 0.05$) decrease for MTS-TAMRA–treated versus nontreated oocytes. There was no significant effect of phlorizin on P_{urea} for oocytes treated with MTS reagents ($P > 0.05$). In this experiment, the phlorizin-sensitive urea uptake for mutant Y290C was 4.0 ± 0.9 pmols/h (n = 9), and the phlorizin-sensitive uptake of αMDG for WT was 136 ± 9 pmols/h (n = 9). **$P < 0.01$; ***$P < 0.001$.

Selectivity of Water/Urea Pathway. The parallel changes in water and urea permeabilities and the effect of MTS reagents on mutants F453C, Q457C, H83C, and Y290C indicate water and urea share a common pathway through hSGLT1. The pathway is much more restrictive for urea than for water, the ratio of the unitary P_f/P_{urea} of 200 and 50 for WT and mutant Q457C. Previous studies showed that glycerol, sulfate, chloride, and L-alanine did not permeate rabbit SGLT1 (7), but ethylene glycol did (28). There was no remarkable divergence of urea and water permeabilities with modifications of side chains (to cysteine or on alkylation of cysteine with MTS reagents; Tables 1 and 2). The selectivity suggests that the limiting radius of the hSGLT1 water channel is less than 2 Å, i.e., slightly wider than that in orthodox water channels (AQP1) that are urea impermeable.

Another major difference between passive water permeation through transporters and aquaporins is that competitive transport inhibitors, phlorizin for SGLT1 and SKF89976A for GAT1, block water, suggesting conformationally dependent water permeation. Our P_f measurements were carried out on the Na^+-bound outward-facing open conformation, whereas the MD simulations on vSGLT were carried out on the sugar-bound, inward-facing occluded conformation. Currently, there are no crystal structures of hSGLT1 in any conformation, and so it is premature to speculate on the structural basis of phlorizin inhibition or conformational changes on water and urea permeation through hSGLT1, especially given the order of magnitude differences in time scale of the MD simulations and the permeability measurements.

Physiological Significance. The interaction between water and SGLT1 is part of the molecular mechanism underlying the energetics of Na^+ and glucose transport across the membrane from one aqueous environment to another. To bypass the energy required to dehydrate glucose (≥12 Kcal/mol), the H bonding between sugar and water, and Na^+ and water, must be exchanged for H bonding to polar side chains of the sugar and Na^+ binding sites. It is not clear whether or not these bond exchanges occur step by step or all at once. Several molecular dynamic simulations show that water in the sugar binding vestibule competes for H bonding with the sugar. The release of sugar and Na^+ into the cytoplasm occurs through an aqueous intramolecular pathway, and Na^+ binding and release from the Na2 site involves exchanges in H bonding between site side chains and water (e.g., refs. 29–32). Whether water molecules will be detected on high-resolution crystal structures of SGLTs remains to be seen. Our studies spotlight the fact that there are aqueous pathways in transporters, and water plays an important structural role in ligand transport, including the binding and release of ligands.

Although the water permeability of SGLT1 is orders of magnitude lower than that for aquaporins, what is important in determining their functional role is the density of the transporters in plasma membranes. In the case of the small intestine, a major site of water absorption and secretion, SGLT1 is abundant in the brush border membrane, whereas orthodox aquaporins are absent. Each day, the human small intestine absorbs 6.5 L of fluid, in the absence of, or even against a bulk osmotic gradient.

Table 2. Effects of MTS reagents on urea permeability of oocytes expressing hSGLT1 proteins P_{urea} (10^{-7} cm·s^{-1})

Expt	Na^+	Pz	MTSEA	MTS-TAMRA
Native	0.43 ± 0.02	0.57 ± 0.02***	0.40 ± 0.03	0.45 ± 0.01
WT	0.83 ± 0.04	0.41 ± 0.03***	0.90 ± 0.04	0.95 ± 0.07
F453C	1.59 ± 0.04	0.34 ± 0.01***	1.45 ± 0.02***	0.71 ± 0.02***
Q457C	1.46 ± 0.03	0.46 ± 0.11***	0.91 ± 0.22***	1.00 ± 0.02***
H83C	1.21 ± 0.05	0.76 ± 0.09***	1.35 ± 0.04	1.18 ± 0.05
Y290C	0.95 ± 0.04	0.56 ± 0.04***	1.14 ± 0.04***	0.72 ± 0.03***
F101C	1.27 ± 0.12	0.59 ± 0.04***	1.01 ± 0.10	1.05 ± 0.11
T287C	1.42 ± 0.03	0.68 ± 0.02***	1.21 ± 0.04***	1.07 ± 0.03***

The experimental protocols were as described in Figs. 4*B* and 5*B*. In each experiment, the contribution of SGLT1 to the total oocyte urea permeability was obtained from the phlorizin-sensitive component. The data shown for each mutant is the mean ± SEM of experiments on nine oocytes for each condition on the same batch of oocytes, see Fig. 4*B* for Y290C and Fig. 5*B* for F453C. Control data were from native oocytes from the same batch used for each mutant. *** highly statistically significant ($P < 0.001$) and ** significant compared with P_{urea} in the absence of phlorizin. The experiments were repeated two to three times for each mutant.

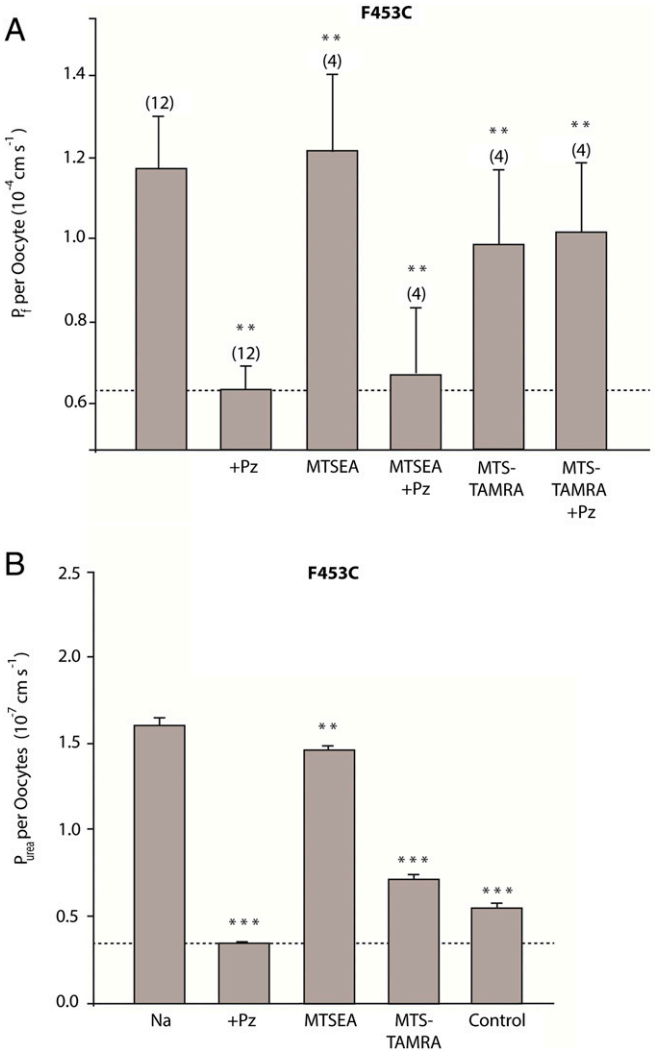

Fig. 5. Effect of MTS reagents on P_f and P_{urea} of oocytes expressing F453C. (*A*) Water permeability of F453C-expressing oocytes. MTSEA had no significant effect on P_f, whereas phlorizin reduced the P_f to those of native oocytes (paired data from four oocytes). MTS-TAMRA decreased P_f significantly compared with controls (four paired experiments), and Pz no longer had any effect in these oocytes. DTT reversed the effect of the MTS-TAMRA (data not shown); it restored the P_f and the Pz effect to within 10% of control. Note that the P_f axis is truncated at 0.5. ** denotes statistically significance ($P < 0.01$) between the experimental condition and the oocyte before MTS treatment. (*B*) P_{urea} of oocytes expressing mutant F453C. In a single experiment, the oocytes were incubated for 2 min in 100 μM MTSEA, or 1 h in 100 μM TMRMTS in 100 mM NaCl buffer. Each error bar is the mean ± SEM ($n = 9$). There was a significant decrease ($P \leq 0.05$) in urea uptakes in the presence of 250 μM phlorizin. There was also a significant decrease in urea permeability after treatment with MTSEA or MTS-TAMRA. ** statistically significant ($P < 0.01$) and *** very highly significant ($P < 0.001$). The control is on native (noninjected) oocytes.

Osmosis plays a key role in passive and solute driven water transport, but as yet, molecular route and mechanism of water flow across the apical and basolateral membranes of the epithelium remains unclear. The proteins hypothesized to be involved in water transport are the Na^+/glucose cotransporter in the apical membrane (2, 4, 13) and the K/Cl cotransporter in the basolateral membrane (5). To examine the relevance of SGLT1 in passive water flow across the intestine, we measured the effect of the specific inhibitor phlorizin on the osmotic flow across the mouse intestine (Fig. 6). We find that phlorizin blocks 65% of the flow, indicating that SGLT1 plays an important role in osmotic flow across the intestine, and water flows through cells and not the paracellular pathway. We anticipate that other transport proteins would also be involved in water transport across the intestine and other membranes. Thus, the water and urea permeabilities of transporters are not just curiosities to structural biologists but are of considerable physiological importance.

Methods

Homology Model. A homology model of hSGLT1 based on the vSGLT structure (PDB ID code 3DH4) is shown in Fig. 1 (24). The sugar binding site is located in the middle of the protein, and when sugar is bound it is isolated from the external and internal membrane surfaces by inner gate Y290, and outer gates F453, F101, and L87. Molecular dynamical studies on vSGLT have indicated that water flows through the sugar pathway (8–11, 31). The water pathway through hSGLT1 is based on the study of vSGLT, where the probability of a residue being within 3 Å of a continuous water chain through vSGLT was obtained (11), and the homologous residues in hSGLT1 were located. The residues include Y87, V126, F453, Q457, D254, Q451, V296, G272, F101, R300, G82, T127, I456, I297, T90, I397, I98, S94, Y153, Y290, H83, T271, S77, T460, S273, K157, S396, I152, and D294. To probe the hSGLT1 water pathway, we examined mutated residues in the sugar pathway between the outer and inner gates to cysteines (H83C, F101C, T287C, Y290C, S392C, Q457C, and F453C) and include a control residue outside the pathway (G507C). Residues lining the inner vestibule, K157, Y153, S392, S396 and R300, have not yet been examined because these residues are not accessible to external MTS reagents, e.g., urea transport by S392C is not sensitive to MTSEA.

Oocytes. WT hSGLT1 and mutant proteins were expressed in *Xenopus laevis* oocytes as described (24, 26). Animal experiments at the University of Copenhagen were performed in accordance with the institutional guidelines mandated by the Danish National Committee for Animal Studies and at University of California, Los Angeles under the approval of the University of California, Los Angeles Animal Research Committee (ARC). *X. laevis* prophase-arrested oocytes were purchased from Ecocyte Bioscience US. Each of the mutant proteins were functional and transported sugar with half-saturation concentration ($K_{0.5}$) values for αMDG ranging from 0.5 mM (for WT, T287C, G507C) to >100 mM (for H83C and Y290C). For all oocytes, the maximal sugar-induced current (I_{max}, at −150 mV) and the total number of transporters were determined (see below).

Water Permeability. Oocytes were placed in an experimental chamber and their volume was monitored via an inverted microscope with light supplied from a Perspex rod (Fig. 2*A*). The osmotic water permeability (P_f) of oocytes was determined at 22 °C by recording the changes in cell volume following step changes in the extracellular osmolarity (2–4, 12, 13, 19). The relative volume of the oocytes (V/V_o) is related to the cross-sectional area A by: $V/V_o = (A/A_o)^{3/2}$, where V is the volume, V_o is the initial volume, and A_o is the initial cross-sectional area. P_f (in units of cm·s^{-1}) is proportional to the rate of change of cell volume: V_o (d/dt V/V_o) = $P_f S V_w \Delta\pi$, where S is the oocyte surface area that includes the microvilli (~0.45 cm^2), V_W is the partial molar volume of water (18 $cm^3 \cdot mol^{-1}$) and $\Delta\pi$ is the osmotic gradient. The contribution of hSGLT1 to the total oocyte P_f was determined by blocking SGLT1 by the specific inhibitor phlorizin, which returns the total passive water permeability to that of the native oocyte (3). The heterologously expressed proteins simply add to the water permeability of the oocyte. Identical values of P_f are obtained from swelling and shrinkage experiments (positive or negative $\Delta\pi$), and P_f was determined from very small (0.002%) changes in oocyte volume (13, 19). Furthermore, coexpression of AQP1 with SGLT1 simply adds to the water permeability of the SGLT1 oocyte and did not alter the P_f values derived for the SGLT (33). These facts rebut the assertion that stretching of the membrane affects P_f measurements in oocytes (22).

Water flow through hSGLT1 was taken as the difference between flows measured before and after the addition of up to 250 μM phlorizin to the extracellular solution (Fig. 2). The competitive, reversible, nontransported SGLT1 inhibitor reduces the water flow to the level of noninjected oocytes (3). The higher-than-usual phlorizin concentration was to ensure complete inhibition of SGLT activity in all mutants, because the inhibitory constant K_i ranged from 0.2 μM for WT hSGLT1 to 37 μM for mutants Y290C and F101C (24).

Osmotic water permeability per SGLT1 molecule or the unitary P_f (in units of $cm^3 \cdot s^{-1}$) was obtained by dividing the phlorizin-sensitive P_f by the density (n/S) of SGLT1 molecules in the oocyte plasma membrane (34). The number (n) of transporters in the oocyte plasma membrane was determined from

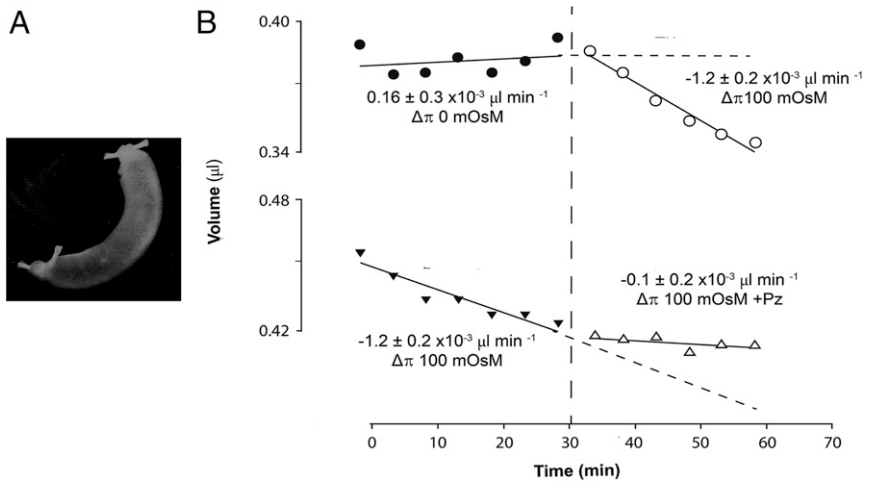

Fig. 6. Water transport across the mouse small intestine. (*A*) Everted sac. The photograph shows a mouse small intestine of length 2.5 cm, everted, with the luminal or apical membrane of the epithelium facing the external solution (150 mM NaCl buffer). The serosal or basolateral membrane surface faces the internal solution (150 mM NaCl buffer). (*B*) Water transport across the everted sac at 22 °C. The upper trace shows the time course of the weight of everted sac before and after an osmotic gradient ($\Delta\pi$) was imposed (at time = 30 min) with the addition of mannitol (100 mM) to the external NaCl buffer. The bottom trace is from an experiment on a different preparation (Δ) where the osmotic gradient was initiated at time 0. Water initially flowed out of the sac into the external solution, and when phlorizin was added to the external solution after 30 min, the osmotic flow was blocked. The rates were obtained by linear regression.

the SGLT1 capacitive currents (12, 24, 26, 35). Briefly, the membrane potential of the oocyte was held at −50 mV and stepped to various test values (from +50 mV to −150 mV) for 100 ms before returning to −50 mV. In the presence of 100 mM Na^+ buffer and the absence of sugar, the total current (I_{tot}) was fitted to $I_{tot}(t) = I_{cm} \exp(-t/\tau_{cm}) + I_{pss} \exp(-t/\tau) + I_{ss}$, where I_{ss} is the steady-state current, $I_{cm} \exp(-t/\tau_{cm})$ is the bilayer capacitive current with initial value I_{cm} and time constant τ_{cm}, and $I_{pss} \exp(-t/\tau)$ is the SGLT1 presteady-state current.

SGLT1 presteady-state current [$I_{pss} \exp(-t/\tau)$] was isolated by subtraction of the capacitive and steady-state components from the total current. At each voltage, charge movement (Q) was obtained by integrating the presteady-state currents. The charge vs. voltage (Q-V) relation was fitted to a Boltzmann equation: $(Q - Q_{hyp})/Q_{max} = 1/[1 + \exp\{(V_m - V_{0.5})zF/RT\}]$, where $Q_{max} = Q_{dep} - Q_{hyp}$, and Q_{dep} and Q_{hyp} are the charge at depolarizing and hyperpolarizing limits, V_m is membrane potential, F is the Faraday constant, R is the gas constant, T is absolute temperature, $V_{0.5}$ is midpoint voltage, and z is the apparent valence of the voltage sensor. The number of transporters (n) in the plasma membrane was calculated from the formula $n = Q_{max}/z{\cdot}e$ where $z \sim 1$ for WT and SGLT1 mutants (12, 26) and e is the elementary charge. We have shown that Q_{max} is proportional to the number of SGLT1 transporters in the plasma membrane: a Q_{max} of 10 nC is equivalent to 1×10^{10} proteins in the oocyte plasma membrane (12). Before each experiment, Q_{max} and S (the oocyte surface area obtained from the membrane capacitance, and is similar to that from electron microscopy; ref. 12) were recorded, and the density (n/S) of WT and mutant proteins expressed in each oocyte was estimated.

Urea Uptake Experiments. Urea uptakes into oocytes were as described (7), except for here we use hSGLT1 and mutants. Uptakes of 55 µM [^{14}C] urea or mannitol, or 50 µM αMDG, were measured at 22 °C for 30 min and expressed in pmoles per oocytes/h. hSGLT1-specific urea uptakes were obtained as the phlorizin-sensitive uptake (250 µM). Uptakes of αMDG were used as an internal control for the expression of SGLT1 mutants in each batch of oocytes.

Urea permeability of oocytes, P_{urea} (cm·s^{-1}), was determined according to $P_{urea} = J_{urea}/([\text{urea}]\ S)$, where J_{urea} is the rate of urea flux (mol·cm^{-2}·s^{-1}), and [urea] is the urea concentration (55×10^{-9} moles·cm^{-3}). Urea permeability per SGLT1 molecule, or unitary P_{urea} (cm^3·s^{-1}), was obtained by dividing the phlorizin-sensitive P_{urea} by the density (n/S) in the oocyte membrane. For these experiments, oocytes with similar levels of expression were used. Eighteen oocytes with Q_{max} in a narrow range were selected, and urea uptakes were measured in the presence and absence of 250 µM phlorizin in NaCl buffer (nine oocytes each). There was no effect of the initial measurement of Q_{max} on urea uptakes through the oocyte membrane or hSGLT1: on one batch of oocytes, urea uptakes were measured in nine with and nine without Q_{max} measurements, $P < 0.001$. The unitary P_{urea} per SGLT1 molecule was obtained from the phlorizin-sensitive urea uptakes. In experiment of Fig. 3*B*, n was estimated from Q_{max} measurements for WT and mutant Q457C. For the other mutants, n was based on our previous estimates of protein expression (24). The Q_{max} values for WT and Q457C were similar to the previous estimates (24).

Everted Sac Technique. The contribution of SGLT1 to water transport across the intestine was studied by using an everted sac method where we monitored the changes in weight of the sac in response to an osmotic gradient across the epithelium (36). The small intestines were isolated from freshly killed adult mice, and the lumen was flushed with ice-cold 150 mM NaCl buffer to remove chime. The small intestine was everted to expose the epithelial cells, and 2.5-cm sacs of midjejunum were filled with 200 µL of a 150 mM NaCl buffer containing 20 mM glucose (serosal solution). The sacs were then incubated in the NaCl buffer at 22 °C and weighed at 5-min intervals for up to 2 h. During the course of the experiment, the mucosal solution was replaced with NaCl buffer containing 100 mM mannitol (with or without 250 µM phlorizin). The NaCl buffer contain the following (in mM): 150 NaCl, 2 KCl, 1 $CaCl_2$, 1 $MgCl_2$, and 10 Tris/Hepes pH 7.4. There is a rich history in the use of in vitro mammalian preparations at 22 °C for the study of passive water, nonelectrolyte, and ion permeation across epithelia such as those of the intestine, gall bladder, and renal tubule. The major advantage is the extended viability of the tissues.

MTS Reagents. $MTSEA^+$ and MTS-TAMRA, (previously known as MTS-TMR), were obtained from Toronto Research Chemicals. Stock solutions were freshly prepared each day in dimethyl sulfoxide (DMSO), and added to NaCl buffer (to 100 µM) immediately before each experiment. The concentrations of DMSO in final buffer did not exceed 1% and had no effect on oocytes expressing SGLTs. Cysteine mutants were labeled by incubating with 100 µM MTSEA for 2 min or 100 µM MTS-TAMRA for 1 h in Na^+ buffer to inhibit SGLT1 sugar currents >80%. The reversibility of MTSEA and MTS-TAMRA effects were examined by treating with 10 mM DTT in NaCl buffer for 5–10 min (Fig. 5*A*).

Na^+/glucose cotransport, monitored as the sugar-induced current, was measured before and after exposure to MTSEA and MTS-TAMRA. For all of the mutants, except the control G507C, the sugar-induced currents were reduced by >80% (see also ref. 24).

Statistical significance was performed by using the paired t test: * denotes significance at ($P < 0.05$), ** highly significant ($P < 0.01$), and *** very highly significant ($P < 0.001$).

ACKNOWLEDGMENTS. We appreciate the advice of Bruce Hirayama throughout this project and the insights provided by Michael Grabe and Joshua Adelman on water permeation through vSGLT. T.Z. is grateful for financial support from the Lundbeck Foundation and the Danish Research Council, and the study has also been supported by NIH Grant DK19567. E.G. was partially supported by a fellowship from the Government of Navarra, Spain.

1. Loike JD, et al. (1996) Sodium-glucose cotransporters display sodium- and phlorizin-dependent water permeability. *Am J Physiol* 271(5 Pt 1):C1774–C1779.
2. Loo DD, Zeuthen T, Chandy G, Wright EM (1996) Cotransport of water by the Na^+/glucose cotransporter. *Proc Natl Acad Sci USA* 93(23):13367–13370.
3. Loo DD, et al. (1999) Passive water and ion transport by cotransporters. *J Physiol* 518(Pt 1):195–202.
4. Zeuthen T, et al. (1997) Water transport by the Na^+/glucose cotransporter under isotonic conditions. *Biol Cell* 89(5-6):307–312.
5. Zeuthen T (2010) Water-transporting proteins. *J Membr Biol* 234(2):57–73.
6. Loo DD, Wright EM, Zeuthen T (2002) Water pumps. *J Physiol* 542(Pt 1):53–60.
7. Leung DW, Loo DD, Hirayama BA, Zeuthen T, Wright EM (2000) Urea transport by cotransporters. *J Physiol* 528(Pt 2):251–257.
8. Choe S, Rosenberg JM, Abramson J, Wright EM, Grabe M (2010) Water Permeation Through the Sodium-Dependent Galactose Cotransporter vSGLT *Biophys J* 99(7):L56–L58.
9. Sasseville LJ, Cuervo JE, Lapointe JY, Noskov SY (2011) The structural pathway for water permeation through sodium-glucose cotransporters. *Biophys J* 101(8):1887–1895.
10. Li J, et al. (2013) Transient formation of water-conducting states in membrane transporters. *Proc Natl Acad Sci USA* 110(19):7696–7701.
11. Adelman JL, et al. (2014) Structural determinants of water permeation through the sodium-galactose transporter vSGLT. *Biophys J* 106(6):1280–1289.
12. Zampighi GA, et al. (1995) A method for determining the unitary functional capacity of cloned channels and transporters expressed in Xenopus laevis oocytes. *J Membr Biol* 148(1):65–78.
13. Meinild A, Klaerke DA, Loo DD, Wright EM, Zeuthen T (1998) The human Na^+-glucose cotransporter is a molecular water pump. *J Physiol* 508(Pt 1):15–21.
14. Meinild AK, Klaerke DA, Zeuthen T (1998) Bidirectional water fluxes and specificity for small hydrophilic molecules in aquaporins 0-5. *J Biol Chem* 273(49):32446–32451.
15. Fischbarg J, et al. (1990) Glucose transporters serve as water channels. *Proc Natl Acad Sci USA* 87(8):3244–3247.
16. Zeuthen T, Zeuthen E, Macaulay N (2007) Water transport by GLUT2 expressed in Xenopus laevis oocytes. *J Physiol* 579(Pt 2):345–361.
17. Hasegawa H, et al. (1992) A multifunctional aqueous channel formed by CFTR. *Science* 258(5087):1477–1479.
18. Meinild AK, Loo DD, Pajor AM, Zeuthen T, Wright EM (2000) Water transport by the renal $Na(^+)$-dicarboxylate cotransporter. *Am J Physiol Renal Physiol* 278(5):F777–F783.
19. Zeuthen T, Belhage B, Zeuthen E (2006) Water transport by Na^+-coupled cotransporters of glucose (SGLT1) and of iodide (NIS). The dependence of substrate size studied at high resolution. *J Physiol* 570(Pt 3):485–499.
20. MacAulay N, Gether U, Klaeke DA, Zeuthen T (2002) Passive water and urea permeability of a human $Na(^+)$-glutamate cotransporter expressed in Xenopus oocytes. *J Physiol* 542(Pt 3):817–828.
21. Zeuthen T, Macaulay N (2012) Cotransport of water by Na^+-K^+-$2Cl^-$ cotransporters expressed in Xenopus oocytes: NKCC1 versus NKCC2. *J Physiol* 590(5):1139–1154.
22. Erokhova L, Horner A, Ollinger N, Siligan C, Pohl P (2016) The sodium glucose co-transporter SGLT1 is an extremely efficient facilitator of passive water transport. *J Biol Chem* 291(18):9712–9720.
23. Faham S, et al. (2008) The crystal structure of a sodium galactose transporter reveals mechanistic insights into Na^+/sugar symport. *Science* 321(5890):810–814.
24. Sala-Rabanal M, et al. (2012) Bridging the gap between structure and kinetics of human SGLT1. *Am J Physiol Cell Physiol* 302(9):C1293–C1305.
25. Jiang X, Loo DD, Hirayama BA, Wright EM (2012) The importance of being aromatic: π interactions in sodium symporters. *Biochemistry* 51(47):9480–9487.
26. Loo DD, Jiang X, Gorraitz E, Hirayama BA, Wright EM (2013) Functional identification and characterization of sodium binding sites in Na symporters. *Proc Natl Acad Sci USA* 110(47):E4557–E4566.
27. Loo DDF, Hirayama BA, Karakossian MH, Meinild AK, Wright EM (2006) Conformational dynamics of hSGLT1 during Na^+/glucose cotransport. *J Gen Physiol* 128(6): 701–720.
28. Panayotova-Heiermann M, Wright EM (2001) Mapping the urea channel through the rabbit $Na(^+)$-glucose cotransporter SGLT1. *J Physiol* 535(Pt 2):419–425.
29. Watanabe A, et al. (2010) The mechanism of sodium and substrate release from the binding pocket of vSGLT. *Nature* 468(7326):988–991.
30. Li J, Tajkhorshid E (2012) A gate-free pathway for substrate release from the inward-facing state of the Na^+-galactose transporter. *Biochim Biophys Acta* 1818(2):263–271.
31. Bisha I, Rodriguez A, Laio A, Magistrato A (2014) Metadynamics simulations reveal a Na^+ independent exiting path of galactose for the inward-facing conformation of vSGLT. *PLOS Comput Biol* 10(12):e1004017.
32. Li J, Wen PC, Moradi M, Tajkhorshid E (2015) Computational characterization of structural dynamics underlying function in active membrane transporters. *Curr Opin Struct Biol* 31:96–105.
33. Zeuthen T, Meinild AK, Loo DD, Wright EM, Klaerke DA (2001) Isotonic transport by the Na^+-glucose cotransporter SGLT1 from humans and rabbit. *J Physiol* 531(Pt 3): 631–644.
34. Finkelstein A (1987) *Water Movement Through Lipid Bilayers, Pores, and Plasma Membranes: Theory and Reality* (John Wiley & Sons, New York).
35. Loo DD, Hazama A, Supplisson S, Turk E, Wright EM (1993) Relaxation kinetics of the Na^+/glucose cotransporter. *Proc Natl Acad Sci USA* 90(12):5767–5771.
36. Smyth DH, Wright EM (1966) Streaming potentials in the rat small intestine. *J Physiol* 182(3):591–602.